Nuclear Physics **A556** (1993) 123–135
North-Holland

NUCLEAR
PHYSICS A

The ^{26}Al(p, γ)^{27}Si reaction at low stellar temperature

A.E. Champagne

Department of Physics and Astronomy, University of North Carolina at Chapel Hill, Chapel Hill, NC 27599, USA
and
Triangle Universities Nuclear Laboratory, Duke University, Durham, NC 27706, USA

B.A. Brown

Department of Physics and Astronomy and National Superconducting Cyclotron Laboratory, Michigan State University, East Lansing, MI 48824, USA

R. Sherr

Department of Physics, Princeton University, Princeton, NJ 08544, USA

Received 17 August 1992
(Revised 9 December 1992)

Abstract: Shell-model calculations have been used to predict the locations of states in ^{27}Si which are analogous to well-studied states in ^{27}Al. From this, we have determined the resonance properties of the known states in ^{27}Si near the ^{26}Al + p threshold. The resulting thermonuclear reaction rate is uncertain by about a factor of ten at low temperatures, but it appears that the ^{26}Al(p, γ)^{27}Si reaction is too slow to destroy a significant amount of ^{26}Al at these temperatures.

1. Introduction

Diffuse emission of 1809 keV gamma rays from the interstellar medium of our galaxy has been attributed to a large equilibrium abundance ($\approx 3M_{\odot}$) of ^{26}Al [refs. [1-4])] which has a half-life of 7.2×10^5 y. Based upon the available thermonuclear reaction rates, there is strong circumstantial evidence which suggests that ^{26}Al is produced at low temperatures which are characteristic of e.g. asymptotic giant branch (AGB) stars or Wolf-Rayet stars [5]). However, no published model calculations for these or other sources succeeds in producing more than a fraction of the observed abundance [6]). This situation may imply that what is observed is the result of contributions from several different types of sources. Alternately, the theoretical difficulty with producing enough ^{26}Al may be a result of incomplete nuclear-reaction input: Although most of the relevant reaction rates have been accurately determined,

Correspondence to: Dr. A.E. Champagne, Department of Physics and Astronomy, University of North Carolina at Chapel Hill, Chapel Hill, NC 27599, USA.

the reaction which destroys ^{26}Al, namely ^{26}Al(p, γ)^{27}Si, has not been studied in sufficient detail. In equilibrium, ^{26}Al will exist not only in its ground state, but in a thermal population of excited states [7]). However, at low temperatures, only the ground state will make a significant contribution to the reaction rate. Direct (p, γ) measurements [8,9]) have been limited to center-of-mass energies in excess of $E_{c.m.}$ = 189 keV and therefore have not probed the energy region of interest for low-temperature nucleosynthesis. Because the MgAl cycle is not closed [10,11]) any new, low-energy resonances which would be strong enough to increase the ^{26}Al destruction rate would make it more difficult to produce enough ^{26}Al with existing stellar models.

Measurements of the ^{28}Si(^{3}He, α)^{27}Si reaction by Schmalbrock *et al.* [12]) and of the ^{27}Al(^{3}He, t)^{27}Si reaction by Wang *et al.* [13]) have located four states between the proton-capture threshold in ^{27}Si and the lowest observed (p, γ) resonance (fig. 1).

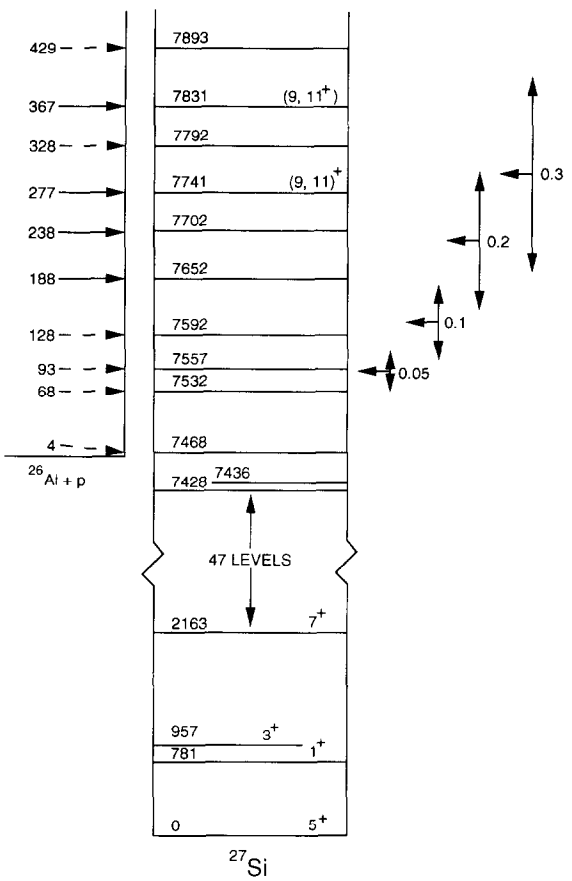

Fig. 1. Level structure of ^{27}Si near the ^{26}Al + p threshold [from ref. [15])]. The locations and widths of the Gamow peak at various temperatures (in units of 10^9 K) are shown to the right. Excitation energies are in units of keV. Spins are listed as 2*J*.

None of these states were observed in a recent measurement [14]) of the $^{26}Al(^{3}He, d)^{27}Si$ reaction because of contaminant states in the region of interest. By assigning analog states in ^{27}Si to three known $J^{\pi} = \frac{9}{2}^{+}$ or $\frac{11}{2}^{+}$ states in ^{27}Al, Wang *et al.* [13]) concluded that only one of these four new states could be formed by s-wave capture. To make these assignments, they used the relative shifts in excitation energy of the four known mirror pairs with $J^{\pi} \geqslant \frac{7}{2}^{+}$ [as compiled by Endt [15])] to constrain the magnitude of the shifts at the higher energies of interest. However, these known mirrors range in excitation energy from 2.2 to 4.5 MeV and therefore do not form an adequate systematic basis to predict mirror pairs at $E_x = 7.5$–8 MeV. To illustrate this point, we show in fig. 2 and table 1 the shifts $\Delta E = E_x(^{27}Si) - E_x(^{27}Al)$ for established positive-parity mirror pairs. Also displayed in fig. 2 are level shifts computed using a single-particle potential model [16]) with a core consisting of $^{26}Al(5^{+})$. The calculations show that level shifts in the region of interest may be as large as −650 keV whereas Wang *et al.* [13]) assumed $\Delta E \approx -100$ keV. However, the observed shifts lie near or above the $1d_{5/2}$ curve in fig. 2. This situation may result from both an absence of $2s_{1/2}$ strength as well as to parentage in higher-lying states in ^{26}Al (which perforce leads to larger binding and higher Coulomb energy).

The nature of the level shifts in $A = 27$ appear to be more complicated than what can be calculated in a naive model. However, using a more realistic calculation of these shifts to predict resonance properties in ^{27}Si is probably more reliable than

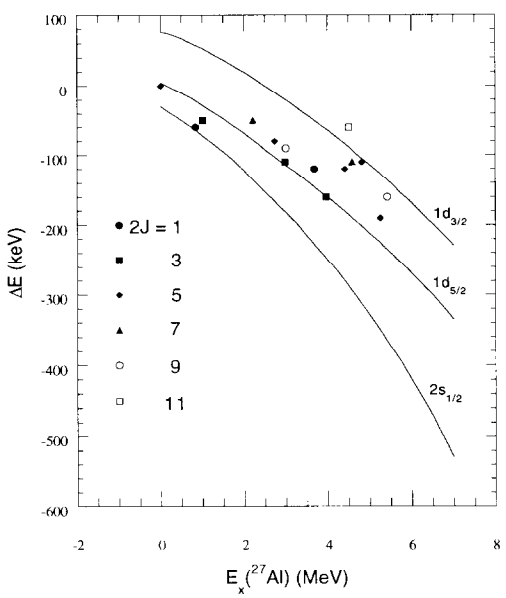

Fig. 2. $A = 27$ energy shifts [defined as $\Delta E = E_x(^{27}Si) - E_x(^{27}Al)$]. The solid curves are theoretical predictions derived from a single-particle potential model.

TABLE 1

Known $A = 27$ mirror states

$2J_n$	$E_x(^{27}Al)$		$E_x(^{27}Si)$			$\delta(\Delta E)$ [e] (keV)
	exp [a] (keV)	calc [b] (keV)	exp (keV)	calc [c] (keV)	calc [d] (keV)	
1_1	844	912	781	825	780	1
1_2	3680	3709	3540	3650	3564	−24
3_1	1014	1264	957	1048	974	−17
3_2	2982	2780	(2866)	2951	2871	−5
3_3	3957	4027	3804	3919	3835	−31
5_1	0	0	0	0	−44	44
5_2	2735	2708	2648	2748	2664	−16
5_3	4410	4139	4289	4417	4301	−12
5_4	4812	4939	4704	4782	4685	19
5_5	5248	5320	5062	5210	5090	−28
7_1	2211	2326	2164	2248	2161	3
7_2	4580	4665	4475	4573	4471	4
9_1	3004	3025	2910	2969	2913	−3
11_1	4510	4584	4447	4491	4385	62

[a]) Experimental values from ref. [15]).

[b]) Calculated using the Wildenthal sd interaction [18]).

[c]) Calculated using Ormand and Brown interaction [19]) for the shift between ^{27}Si and ^{27}Al.

[d]) Corrected values (as described in the text) using $\varepsilon_1 = 20\ (35)$, $\varepsilon_2 = -55\ (15)$, $\varepsilon_3 = -66\ (45)$ and $\gamma = -12.4\ (3.9)$.

[e]) Defined as $E_x(^{27}Si)_{exp} - E_x(^{27}Si)_{calc}$.

simply calculating these properties outright: The former procedure is a straightforward perturbation of the known spectrum of ^{27}Al rather than a construction of ^{27}Si from scratch. To account for the possibility of mixed configurations, we initially used shell-model computations of neutron and proton occupation numbers in the various $T = \frac{1}{2}$, positive-parity states of ^{27}Al to find the fractional numbers of $1d_{5/2}$, $1d_{3/2}$ and $2s_{1/2}$ neutrons which are changed into protons for ^{27}Si. These were multiplied by the computed single-particle shifts (in fig. 2) to find the total shift. Because this technique ignores any parentage in excited states of ^{27}Si, a second type of calculation was performed. Fractional parentage coefficients were used to calculate level shifts for states in which a neutron (proton) of the appropriate j was coupled to various states in ^{26}Al. The weighted-average shift was then determined. While preferred theoretically, it was impractical to carry out this sort of calculation with the necessary completeness. Furthermore, both methods ignore shifts caused by nuclear forces. Consequently, we present here a hybrid model from which we ultimately obtain the resonant and nonresonant contributions to the $^{26}Al(p, \gamma)^{27}Si$ reaction rate.

2. Model for level shifts

The positive-parity levels of ^{27}Al were calculated with the shell-model code OXBASH [17]) using USD matrix elements for the W-interaction in the 2s1d model space [18]). The predicted excitation energies for the states in ^{27}Al with known mirror states are listed in table 1 along with experimental values. While differences are occasionally as large as 200 keV, there is no ambiguity in identifying the appropriate model state. The energies of the ^{27}Si analogs (also listed in table 1) were obtained using the global empirical isospin-nonconserving interactions of Ormand and Brown [19]). The differences between predicted and actual energies are as large as 148 keV, but multiparticle, state-dependent binding-energy effects have not been included at this point.

As it is not possible to use the actual ^{26}Al parents with their correspondingly different binding effects, we assume that there will be a shift for each orbital averaged over the many parents that will be roughly constant for the various states. We also include a dependence on binding (excitation) energy which we assume to be l-independent for the sake of simplicity (in fact the 2s dependence is steeper than for the 1d orbitals). A final correction to account for mixed configurations was made by first calculating the fraction of $2s_{1/2}$, $1d_{5/2}$ and $1d_{3/2}$ orbitals describing the odd neutron in ^{27}Al. For each orbital we ascribe a residual energy shift ε_{2j}. The correction factor for the calculated energy shift for state i can be expressed as

$$\delta(\Delta E)_i = \varepsilon_1 \alpha_1^{(i)} + \varepsilon_5 \alpha_5^{(i)} + \varepsilon_3 \alpha_3^{(i)} + \gamma E_i(^{27}\mathrm{Al}) ,$$

where α_{2j} is the mixing fraction and γ is an empirical parameter. The parameters ε_{2j} and γ were determined by a least-squares fit to the level shifts for the states listed in table 1 (in table 1 and throughout this article, orbitals will be referred to by $2J_n$, i.e. the nth state with spin J). The r.m.s. deviation between the actual shifts and our final predictions is 26 keV. Because the correction factor $\delta(\Delta E)_i$ does not seem to possess an obvious dependence on E_x or J, we used these same parameters to predict the locations of the low-lying ^{26}Al + p resonances.

At the higher energies of interest, the increased level density makes it difficult to assign a unique model orbital to each level (fig. 3). However, by using the expected accuracy of the predicted excitation energy (about ±200 keV) and the known spin information, for the ambiguous cases it is possible to limit assignments to one of two orbitals (as summarized in table 2).

Analog shifts were calculated via the procedure outlined above. To be conservative, each predicted energy shift was assigned a systematic uncertainty of ±50 keV (i.e. double the r.m.s. error at lower excitation energies). The corresponding states in ^{27}Si whose excitation energies fall within our predicted ranges are listed in table 2. For each state in ^{27}Al, there are several proposed, mutually exclusive, analog assignments. In other words, with each known state near the ^{26}Al + p threshold, we can associate several possible model configurations (listed in table 3). This ambiguity will naturally lead to some uncertainty in our final calculation of the reaction rate.

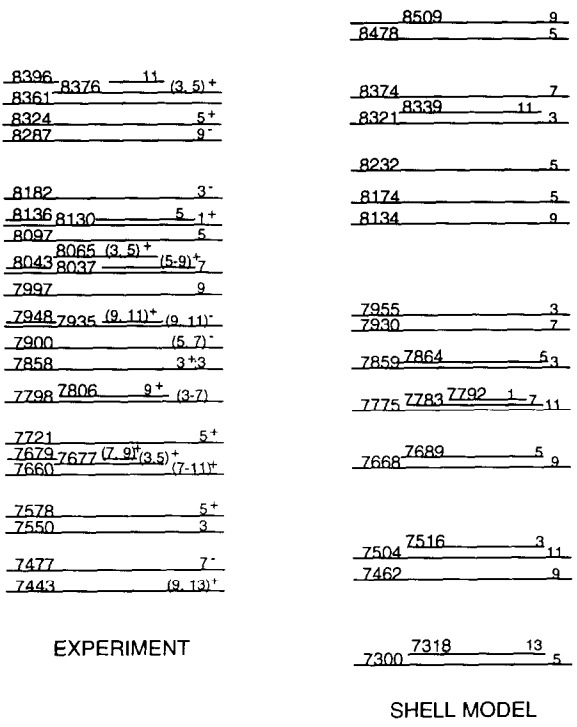

Fig. 3. Levels in ^{27}Al which could be analogous to astrophysically interesting states in ^{27}Si. On the left side are known states tabulated in ref. [15]). The right side shows shell-model predictions for positive-parity states. Spins are denoted by $2J$.

3. Calculation of the reaction rate

3.1. NARROW RESONANCES

The thermonuclear reaction rate is the product of the cross section σ and center-of-mass velocity v, averaged over a maxwellian velocity distribution:

$$\langle \sigma v \rangle = \left(\frac{8}{\pi \mu} \right)^{1/2} (kT)^{-3/2} \int \sigma(E) \exp(-E/kT) \, \mathrm{dE} .$$

For isolated, narrow resonances, the rate may be approximated by

$$\langle \sigma v \rangle = \left(\frac{2\pi}{\mu kT} \right)^{3/2} \hbar^2 \omega\gamma \exp(-E_i/kT) ,$$

where $\omega\gamma$ is the resonance strength defined by

$$\omega = \frac{(2J_r+1)}{(2J_i+1)(2J_t+1)}, \qquad \gamma = \frac{\Gamma_p \Gamma_\gamma}{\Gamma} .$$

TABLE 2

Predicted mirror states

E_x (^{27}Al) [a] (keV)	$2J$ [a]	Possible shell-model configuration assignment [b]	Possible analog state in ^{27}Si [c]
7578	5	5_{11}	7260, 7276, 7324, 7341
7660	(7-11)	$11_3, 9_7$	7383, 7428, 7436, 7468
7677	(3, 5)	3_9	7324, 7341, 7383
7679	(7, 9)	$9_7, 7_{10}$	7341, 7383, 7428, 7436, 7468
7721	5	5_{12}	7468, 7532, 7557
7798	(3-7)	$7_{10}, 7_{11}$	7468, 7532, 7557
7806	9	9_8	7557, 7592, 7652
7948	(9, 11)	$11_4, 9_9, 9_8$	7741, 7831
7997	9	$9_9, 9_8$	7741, 7831
8037	7	$7_{11}, 7_{12}$	7690, 7702, 7789, 7792
8043	(5-9)	$5_{13}, 5_{14}, 7_{11}, 7_{12}, 9_9$	7792, 7831, 7893
8065	(3, 5)	3_{10}	7577, 7592, 7652

[a]) Ref. [15]).

[b]) The first value listed is preferred on the basis of excitation energy.

[c]) Excitation energies from ref. [15]).

Here J_f, J_i and J_t refer to the spins of the final state, target and projectile, respectively, and Γ_p, Γ_γ and Γ are the proton and gamma-ray partial widths and the total width, respectively. At low energies (temperatures), $\Gamma_\gamma \gg \Gamma_p$ and the resonance strength reduces to $\omega\gamma \simeq \omega\Gamma_p$.

In the present case, we are dealing with resonances at $E_{c.m.} = 4$, 68, 93 and 128 keV, all of which qualify as low energy, isolated and narrow. The spin statistical factor is determined by the choice of model orbital. Proton widths were derived from s- and d-wave spectroscopic factors calculated with our shell-model wavefunctions (table 3) and the familiar relation $\Gamma_p = S\Gamma_{s.p.}$, where S is the spectroscopic factor and $\Gamma_{s.p.}$ is the proton width of a (fictitious) pure single-particle state. These widths were obtained from a calculation of the cross section for resonant scattering from a Coulomb plus Woods-Saxon potential. The resulting resonance strengths are listed in table 3 for the four resonances of interest as well as for the lowest observed resonances. The possible g-wave orbitals yield strengths which are negligibly small because of barrier-penetrability considerations. With the exception of the 188 keV resonance, particular choices of orbitals yield strengths that are consistent with experiment. However, the 277 and 367 keV resonances seem to require the same orbital, 9_8. Thus it is clear that we cannot predict a particular resonance strength, but rather a range of values that includes the measured value.

We have not accounted for any possible p-wave resonances amongst the states of interest. The two known negative-parity mirrors display small, positive energy shifts [where $\Delta E = E_x(^{27}\text{Si}) - E_x(^{27}\text{Al})$] which would be expected if these states were predominantly hole states in character. At higher energies, there are three negative-parity states in ^{27}Al which warrant scrutiny: With a positive energy shift, the 7477 keV

TABLE 3

Predicted $^{26}Al+p$ resonance strengths

$E_x(^{27}Si)$ [a] (keV)	$E_{c.m.}$ (keV)	$2J$ [a]	Shell-model configuration assignment	S	$\omega\gamma_{(calc)}$ [b] (eV)	$\omega\gamma$(lit) [c]
7468	4		5_{12}	9×10^{-3}	-	$<1.8\times10^{-63}$ [d])
			7_{10}	0.12	-	
			7_{11}	8.5×10^{-3}	-	
			9_7	0.034, 0.037	2.9×10^{-79}	
			11_3	0.26, 0.72	2.7×10^{-78}	
7532	68		7_{10}	0.12	2.9×10^{-15}	$<2.3\times10^{-13}$ [d])
			7_{11}	8.5×10^{-3}	2.0×10^{-16}	
			9_7	0.034, 0.037	2.2×10^{-13}	
7557	93		3_{10}	-	-	$<1.9\times10^{-10}$ [d])
			7_{10}	0.12	3.4×10^{-12}	
			7_{11}	8.5×10^{-3}	2.3×10^{-13}	
			9_8	7×10^{-4}, 0.063	5.3×10^{-11}	
7592	128		3_{10}	-	-	$<5.7\times10^{-6}$ [d]), $<2.3\times10^{-8}$ [e])
			9_8	7×10^{-4}, 0.063	2.4×10^{-8}	
7652	188		3_{10}	-	-	$5.5\,(9)\times10^{-5}$
			9_8	7×10^{-4}, 0.063	1.6×10^{-6}	
7702	238		7_{11}	8.5×10^{-3}	4.3×10^{-6}	$10\,(5)\times10^{-6}$
			7_{12}	0.010	5.0×10^{-6}	
7741	277	(9, 11)	11_4	0.045, 0.13	0.014	$2.9\,(3)\times10^{-3}$
			9_8	7×10^{-4}, 0.063	1.9×10^{-3}	
			9_9	7×10^{-4}, 0.021	2.0×10^{-3}	
7792	328		7_{11}	8.5×10^{-3}	1.9×10^{-4}	
			7_{12}	0.010	2.2×10^{-4}	
7831	367	(9, 11)	9_8	7×10^{-4}, 0.063	0.042	0.069 (7)
			9_9	7×10^{-4}, 0.021	4.5×10^{-3}	

[a]) Ref. [15]).
[b]) $\omega\gamma_{calc}=(\omega\Gamma_p)_{2s}+(\omega\Gamma_p)_{1d}$.
[c]) Ref. [9]), unless otherwise noted.
[d]) Ref. [13]).
[e]) Ref. [14]).

state ($2J^\pi=7^-$) could be analogous to any of the states of interest. However, a positive shift would be consistent with a hole state rather than a single-particle state and this would imply a weak (p, γ) resonance. On the other hand, both the 7900 keV [$(5, 7)^-$] and 7935 keV [$(9, 11)^-$] states could shift down into the region of interest and appear as strong p-wave resonances in ^{27}Si. Although our calculation ignores this possibility, it does predict that the lowest three resonances are either s- or d-wave and that the 128 keV resonance is either s-wave or negligible. Therefore, unless these states are found to have pathologically large $l=1$ spectroscopic factors, any p-wave resonance strengths should fall within the range of our predictions.

The thermonuclear reaction rate has been calculated for all possible, self-consistent combinations of model orbitals for the lowest four resonances. In all cases, the

4 keV resonance was found to be insignificant. For the three remaining resonances at 68, 93 and 128 keV, respective orbital assignments of 7_{10}, 7_{11} and 3_{10} produced a lower bound on the rate. An upper bound was obtained with s-wave resonances at 68 (9_7) and 128 (9_8) keV. Here the 93 keV resonance was also found to be unimportant. The resulting analytic expressions for these rates are

$$N_A\langle\sigma v\rangle_{low} = 4.67\times10^{-10}T_9^{-3/2}\exp(-0.789/T_9) + 3.71\times10^{-8}T_9^{-3/2}\exp(-1.079/T_9),$$

$$N_A\langle\sigma v\rangle_{high} = 3.54\times10^{-8}T_9^{-3/2}\exp(-0.789/T_9) + 3.87\times10^{-3}T_9^{-3/2}\exp(-1.485/T_9),$$

where T_9 is the temperature in units of 10^9 K. The first term in each limit represents the contribution of the 68 keV resonance. The second terms represent the 93 (low) and 128 keV (high) resonances. In addition, the rate for the higher-energy resonances [from ref. [9])] is

$$N_A\langle\sigma v\rangle = 8.97T_9^{-3/2}\exp(-2.191/T_9) + 473T_9^{-3/2}\exp(-3.220/T_9) + 7763/T_9\exp(-3.944/T_9).$$

These rates are shown in fig. 4 and are listed in table 4.

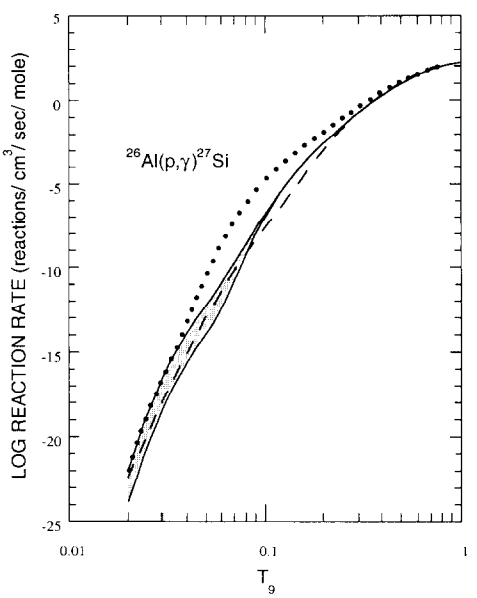

Fig. 4. The $^{26}Al(p, \gamma)^{27}Si$ reaction rate as a function of temperature. The present results are represented by the solid curves. The shaded area denotes the uncertainty in our calculations at low temperatures. The dashed and dotted curves are the rates tabulated by Caughlan and Fowler [21]) and the upper limit of Wang *et al.* [14]), respectively.

TABLE 4

Reaction rates for ^{26}Al(p, γ)^{27}Si

T_9	$N_A\langle\sigma v\rangle$ (cm^3 s^{-1} mole^{-1})							
	non-res	$E_r < 188$ keV		$E_r \geq 188$ keV [a]	Sum		Literature	
		low	high		low	high	[b]	[c]
2.00 $E-02$	1.27 $E-25$	1.22 $E-24$	9.23 $E-23$	8.40 $E-45$	1.35 $E-24$	9.23 $E-23$	4.44 $E-23$	5.37 $E-23$
3.00 $E-02$	2.99 $E-21$	3.42 $E-19$	2.58 $E-17$	3.30 $E-29$	3.45 $E-19$	2.58 $E-17$	1.51 $E-18$	1.98 $E-17$
4.00 $E-02$	1.64 $E-18$	1.67 $E-16$	1.20 $E-14$	1.82 $E-21$	1.69 $E-16$	1.20 $E-14$	1.05 $E-15$	3.71 $E-14$
5.00 $E-02$	1.42 $E-16$	7.27 $E-15$	4.88 $E-13$	7.47 $E-17$	7.48 $E-15$	4.88 $E-13$	1.08 $E-13$	2.22 $E-11$
6.00 $E-02$	4.18 $E-15$	1.01 $E-13$	9.37 $E-12$	8.44 $E-14$	1.90 $E-13$	9.45 $E-12$	3.61 $E-12$	2.01 $E-09$
7.00 $E-02$	6.17 $E-14$	7.26 $E-13$	1.52 $E-10$	1.24 $E-11$	1.31 $E-11$	1.64 $E-10$	5.88 $E-11$	5.00 $E-08$
8.00 $E-02$	5.63 $E-13$	3.35 $E-12$	1.56 $E-09$	5.06 $E-10$	5.11 $E-10$	2.07 $E-09$	5.81 $E-10$	5.44 $E-07$
9.00 $E-02$	3.62 $E-12$	1.12 $E-11$	9.96 $E-09$	8.89 $E-09$	8.91 $E-09$	1.89 $E-08$	4.00 $E-09$	3.42 $E-06$
1.00 $E-01$	1.79 $E-11$	2.97 $E-11$	4.38 $E-08$	8.67 $E-08$	8.68 $E-08$	1.31 $E-07$	2.10 $E-08$	1.47 $E-05$
1.20 $E-01$	2.47 $E-10$	1.27 $E-10$	3.93 $E-07$	2.56 $E-06$	2.56 $E-06$	2.96 $E-06$	3.48 $E-07$	1.28 $E-04$
1.40 $E-01$	1.98 $E-09$	3.50 $E-10$	1.83 $E-06$	2.83 $E-05$	2.83 $E-05$	3.01 $E-05$	4.01 $E-06$	6.04 $E-04$
1.60 $E-01$	1.09 $E-08$	7.36 $E-10$	5.62 $E-06$	1.73 $E-04$	1.73 $E-04$	1.78 $E-04$	3.53 $E-05$	2.03 $E-03$
1.80 $E-01$	4.58 $E-08$	1.29 $E-09$	1.32 $E-05$	7.26 $E-04$	7.26 $E-04$	7.39 $E-04$	2.27 $E-04$	5.64 $E-03$
2.00 $E-01$	1.57 $E-07$	1.98 $E-09$	2.57 $E-05$	2.40 $E-03$	2.40 $E-03$	2.42 $E-03$	1.08 $E-03$	1.40 $E-02$
2.20 $E-01$	4.58 $E-07$	2.79 $E-09$	4.38 $E-05$	6.71 $E-03$	6.71 $E-03$	6.75 $E-03$	4.02 $E-03$	3.19 $E-02$
2.40 $E-01$	1.18 $E-06$	3.67 $E-09$	6.75 $E-05$	1.66 $E-02$	1.66 $E-02$	1.67 $E-02$	1.23 $E-02$	6.75 $E-02$
2.60 $E-01$	2.73 $E-06$	4.58 $E-09$	9.63 $E-05$	3.74 $E-02$	3.74 $E-02$	3.75 $E-02$	3.20 $E-02$	1.33 $E-01$
2.80 $E-01$	5.81 $E-06$	5.50 $E-09$	1.30 $E-04$	7.77 $E-02$	7.77 $E-02$	7.78 $E-02$	7.35 $E-02$	2.46 $E-01$
3.00 $E-01$	1.15 $E-05$	6.39 $E-09$	1.66 $E-04$	1.50 $E-01$	1.50 $E-01$	1.50 $E-01$	1.52 $E-01$	4.27 $E-01$
3.50 $E-01$	4.97 $E-05$	8.45 $E-09$	2.68 $E-04$	5.97 $E-01$	5.97 $E-01$	5.97 $E-01$	6.69 $E-01$	1.37 $E+00$
4.00 $E-01$	1.65 $E-04$	1.01 $E-08$	3.73 $E-04$	1.76 $E+00$	1.76 $E+00$	1.76 $E+00$	2.07 $E+00$	3.48 $E+00$
4.50 $E-01$	4.49 $E-04$	1.14 $E-08$	4.72 $E-04$	4.15 $E+00$	4.15 $E+00$	4.15 $E+00$	5.03 $E+00$	7.35 $E+00$
5.00 $E-01$	1.06 $E-03$	1.24 $E-08$	5.60 $E-04$	8.28 $E+00$	8.28 $E+00$	8.28 $E+00$	1.03 $E+01$	1.36 $E+01$
6.00 $E-01$	4.31 $E-03$	1.35 $E-08$	6.96 $E-04$	2.33 $E+01$	2.33 $E+01$	2.33 $E+01$	3.02 $E+01$	3.43 $E+01$
7.00 $E-01$	1.30 $E-02$	1.38 $E-08$	7.82 $E-04$	4.84 $E+01$	4.84 $E+01$	4.84 $E+01$	6.46 $E+01$	6.64 $E+01$
8.00 $E-01$	3.21 $E-02$	1.37 $E-08$	8.47 $E-04$	8.27 $E+01$	8.27 $E+01$	8.27 $E+01$	1.12 $E+02$	1.08 $E+02$
9.00 $E-01$	6.82 $E-02$	1.33 $E-08$	8.39 $E-04$	1.24 $E+02$	1.24 $E+02$	1.24 $E+02$	1.66 $E+02$	1.56 $E+02$
1.00 $E+00$	1.30 $E-01$	1.28 $E-08$	8.85 $E-04$	1.70 $E+02$	1.70 $E+02$	1.70 $E+02$	2.10 $E+02$	2.07 $E+02$

[a]) Ref. [9]). [b]) Ref. [21]). [c]) Ref. [13]).

3.2. NON-RESONANT CAPTURE

At any given temperature, the ^{26}Al(p, γ)^{27}Si reaction may proceed via direct capture (DC) and through the tails of high-energy or sub-threshold resonances. In general, these non-resonant contributions are insignificant if there are local resonances at stellar energies, as is the case for ^{27}Si. For example, the fact that an s-wave resonance at 4 keV has no significant influence on the reaction rate would seem to imply that resonances at -28 and -36 keV may also be neglected. Consequently, we have ignored any contributions from resonance tails. However, we have calculated the DC rate using the single-particle potential model of Rolfs [20]), but with realistic, diffuse potentials (rather than square wells) for the incident particle and final bound state. In this model, the bound states are treated as single-particle states. We then multiply the cross sections to individual final states by our calculated spectroscopic factors to obtain the total DC cross section. Because our calculation is limited to positive-parity states, we cannot treat El capture to any negative-parity states. Fortunately, there are few negative-parity bound states in ^{27}Si and none below $E_x = 4055$ keV. Therefore, we do not expect that the omission of these states will lead to a gross underestimate of the DC cross section. From this calculation, we have obtained the following approximate analytic expression for the DC rate:

$$N_A\langle\sigma v\rangle_{DC} = 1.53 \times 10^9 T_9^{-1.75} \exp\left(-23.19/T_9^{1/3}\right).$$

This contribution to the reaction rate is also negligible for temperatures greater than about $T_9 = 0.02$.

4. Conclusions

At temperatures $T_9 \leq 0.08$, our present rate for the ^{26}Al(p, γ)^{27}Si reaction does not differ dramatically from what has been tabulated by Caughlan and Fowler [21]) (fig. 4 and table 4), which was based upon different resonance strengths (note that there are minor differences between their tabulated rate and their analytic expression for the rate). However, we believe that our 1–2 order-of-magnitude uncertainty at low temperatures is generally representative of the quality of estimates of this rate. Our upper limit for $T_9 > 0.03$ is 1–2 orders of magnitude lower than that of Wang *et al.*[13]), primarily because they assumed proton widths for their resonances which were equivalent to single-particle estimates whereas we made use of our calculated spectroscopic factors in determining widths. For temperatures $T_9 \geq 0.1$, we recommend the experimentally derived rate of Vogelaar *et al.*[9]) rather than the tabulated [21]) rate. For $T_9 < 0.1$, the large uncertainty in the rate does not necessarily result in an equally large uncertainty in the net abundance of ^{26}Al because its production rate is comparable to a typical burning lifetime. In other words, the abundance of ^{26}Al builds up slowly enough so that only a small fraction can be destroyed before burning ceases. We illustrate this situation in a schematic fashion

for the case of hot-bottom burning in intermediate-mass AGB stars. In these stars energy is provided by thin hydrogen- and helium-burning shells. The latter shell burns in a series of pulses and can produce ^{25}Mg via the sequence $^{14}N(\alpha, \gamma)^{18}F(\beta^+)^{18}O(\alpha, \gamma)^{22}Ne(\alpha, n)^{25}Mg$. Between pulses, we assume that the ^{25}Mg will be mixed into the envelope where it will be converted into ^{26}Al via a (p, γ) reaction. As the star ages, the temperature at the base of the envelope will increase and the interpulse period will decrease (a consequence of an increasing core mass). Production of ^{26}Al will occur if this temperature exceeds $T_9 = 0.04$.

In fig. 5 we show the *net* amount of ^{26}Al (expressed as a fraction of the initial ^{25}Mg abundance) produced as a function of time. This calculation was performed at constant temperature and density ($\rho = 1$ g/cm^3, mass fraction of hydrogen = 0.7) and therefore ignores the effect of convection in the envelope. However, it illustrates the result of an uncertain $^{26}Al(p, \gamma)^{27}Si$ rate: For $T_9 = 0.04$, this rate is small compared to the beta-decay rate and hence there is an insignificant uncertainty in the (small) amount of ^{26}Al produced. Its abundance grows almost linearly with time because the beta-decay rate is much slower than the production rate. At $T_9 = 0.06$, ^{26}Al is produced more rapidly, but destruction is also more efficient and this causes the abundance curve to flatten out with time. Here the interpulse period is on the order of 10^3 yr [ref. [22])] after which the uncertainty in the ^{26}Al abundance is only 14%. However, at $T_9 = 0.08$, where the interpulse period drops to a few hundred years,

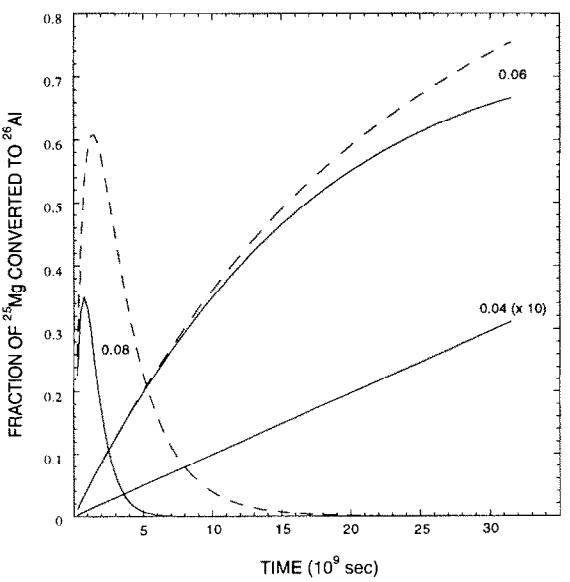

Fig. 5. The amount of ^{26}Al (expressed as a fraction of the initial ^{25}Mg abundance) converted into ^{27}Si as a function of burning time for temperatures $T_9 = 0.04$, 0.06 and 0.08. The dashed and solid lines refer to upper and lower limits (which correspond to lower and upper limits on the rate of the $^{26}Al(p, \gamma)^{27}Si$ reaction), respectively. Constant temperature and density are assumed.

the final abundance of ^{26}Al depends more heavily on the ^{26}Al(p, γ) rate (which is uncertain by a factor of 4). The abundance quickly reaches a maximum at the point where all of the initial ^{25}Mg is exhausted. The amount of ^{26}Al surviving past this time depends solely on its destruction rate. When convection is included, the uncertainty in ^{26}Al production will be less dramatic (simply because the material will spend an appreciable fraction of the burning time at lower temperatures), but will still amount to at least a factor of 2.

It appears that the ^{26}Al(p, γ)^{27}Si reaction rate is low enough to insure that ^{26}Al will survive at low stellar temperatures. Although we have shown that reasonably accurate predictions of the ^{26}Al abundance may be made despite the large uncertainty in its destruction rate, more accurate results are clearly desirable. Experimentally determined analog assignments would be useful, but an improved ^{26}Al(^{3}He, d)^{27}Si measurement is obviously called for. Work in this direction is in progress.

We would like to thank M. Betterton and Z.Q. Mao for their help with these computations. Also, we would like to thank B.H. Wildenthal for his calculation of several spectroscopic factors. This work was supported in part by the U.S. Department of Energy (contract #DE-FG05-88ER40442) and in part by the National Science Foundation (contract #PHY90-17077 and #PHY91-04414).

References

1) W.A. Mahoney, J.C. Ling, W.A. Wheaton and A.S. Jacobson, Astrophys. J. **286** (1984) 578
2) G.H. Share, R.L. Kinzer, J.D. Kurfess, E.L. Chupp and E. Rieger, Astrophys. J. **292** (1985) L61
3) C.J. MacCallum, A.F. Huters, P.D. Stang and M. Leventhal, Astrophys. J. **317** (1987) 877
4) P. von Ballmoos, R. Diehl and V. Schönfelder, Astrophys. J. **318** (1987) 654
5) Ch. Iliadis, Th. Schange, C. Rolfs, U. Schröder, E. Somorjai, H.P. Trautvetter, K. Wolke, P.M. Endt, S.W. Kikstra, A.E. Champagne, M. Arnould and G. Paulus, Nucl. Phys. **A512** (1990) 509
6) R. Ramaty and N. Prantzos, Comments Astrophys. **15** (1991) 301
7) R.A. Ward and W.A. Fowler, Astrophys. J. **238** (1980) 266
8) L. Buchmann, H. Hilgemeier, A. Krauss, A. Redder, C. Rolfs, H.P. Trautvetter and T.R. Donoghue, Nucl. Phys. **A415** (1984) 93
9) R.B Vogelaar, L.W. Mitchell, R.W. Kavanagh and H.A. O'Brien, to be submitted to Phys. Rev.
10) R. Timmermann, H.W. Becker, C. Rolfs, U. Schröder and H.P. Trautvetter, Nucl. Phys. **A477** (1988) 105
11) A.E. Champagne, C.H. Cella, R.T. Kouzes, M.M. Lowry, P.V. Magnus, M.S. Smith and Z.Q. Mao, Nucl. Phys. **A487** (1988) 433
12) P. Schmalbrock, T.R. Donoghue, M. Wiescher, V. Wijekumar, C.P. Browne, A.A. Rollefson, C. Rolfs and A. Vlieks, Nucl. Phys. **A457** (1986) 182
13) T.F. Wang, A.E. Champagne, J.D. Hadden, P.V. Magnus, M.S. Smith, A.J. Howard and P.D. Parker, Nucl. Phys. **A499** (1989) 546
14) R.B. Vogelaar, L.W. Mitchell, R.W. Kavanagh, A.E. Champagne, P.V. Magnus, M.S. Smith, A.J. Howard, P.D. Parker and H.A. O'Brien, to be submitted to Phys. Rev.
15) P.M. Endt, Nucl. Phys. **A521** (1990) 1
16) R. Sherr and G. Bertsch, Phys. Rev. **C32** (1985) 1809
17) B.A. Brown, A. Etchegoyen and W.D.M. Rae, MSU/NSCL Report **524** (1985)
18) B.A. Brown and B.H. Wildenthal, Ann. Rev. Nucl. Part. Sci. **38** (1988) 29
19) W.E. Ormand and B.A. Brown, Nucl. Phys. **A491** (1989) 1
20) C. Rolfs, Nucl. Phys. **A217** (1973) 29
21) G.R. Caughlan and W.A. Fowler, At. Data Nucl. Data Tables **40** (1988) 284
22) I. Iben Jr. and A. Renzini, Phys. Reports **105** (1984) 329